N^2-Hydroxyguanosine 5′-Monophosphate Is a Time-Dependent Inhibitor of *Escherichia coli* Guanosine Monophosphate Synthetase†

Michael L. Deras,‡,§ Sridar V. Chittur,‡ and V. Jo Davisson*

Department of Medicinal Chemistry and Molecular Pharmacology, Purdue University, West Lafayette, Indiana 47907-1333

Received August 17, 1998; Revised Manuscript Received October 14, 1998

ABSTRACT: In contrast to several other glutamine amidotransferases including asparagine synthetase, cytidine 5′-triphosphate (CTP) synthetase, carbamoyl phosphate synthetase, and phosphoribosyl pyrophosphate (PRPP) amidotransferase, guanosine monophosphate synthetase (GMPS) will not utilize hydroxylamine as an alternative nitrogen source. Instead, the enzyme is inhibited by an unknown mechanism. One untested hypothesis was that hydroxylamine serves as a substrate and intercepts a xanthosine 5′-monophosphate-(XMP-) adenylate intermediate in the enzyme active site. The nucleotide product of this substitution reaction would be N^2-hydroxyguanosine 5′-monophosphate (N^2-OH-GMP, **2**). Here we describe the chemoenzymatic preparation of **2**, via the nucleotide 2-fluoroinosine 5′-monophosphate (F-IMP, **5**), and characterization of both these compounds as inhibitors of *Escherichia coli* GMPS. F-IMP was conceived as an electronic mimic of a reactive intermediate in the GMPS reaction but was found to bind weakly to the enzyme (IC_{50} > 2 mM). In contrast, N^2−OH-GMP shows time-dependent inhibition and is competitive with respect to XMP (K_i = 92 nM), representing the first example of a compound that displays these kinetic properties with GMPS. The mechanism of inhibition is proposed to occur via formation of a ternary E·ATP·**2** complex, followed by a rate-determining isomerization to a higher affinity complex that has a $t_{1/2}$ =7.5 min. The contrast in inhibitory activity for 2-substituted purines with GMPS formulates a basis for future inhibitor design. In addition, these results complement recent structural studies of GMPS and implicate the formation of the XMP−adenylate intermediate inducing a probable conformational change that stimulates the hydrolysis of glutamine.

The 12 steps of de novo purine biosynthesis ultimately produce AMP and GMP and are common to all known organisms except ciliates (*1*, *2*). This pathway provides precursors of DNA, RNA, second messengers, and metabolic energy equivalents. Expression levels of several purine biosynthetic enzymes are elevated in neoplastic cell lines as measured by in vivo activity, and conversely, genes coding for enzymes that degrade purines are repressed (*3*). Purines have also been shown to be required for T-cell proliferation, because these cells lack purine salvage pathways, and represent a basis for selective immunomodulation strategies (*4*−*6*). Antimetabolites targeting various aspects of de novo purine biosynthesis have been available for some time, yet more selective and less toxic agents are desired (*7*−*10*).

Guanosine monophosphate synthetase (GMPS,[1] EC 6.3.5.2) catalyzes the last step in the G-branch of purine biosynthesis, converting XMP to GMP (Figure 1). The reaction catalyzed by GMPS requires XMP, magnesium, an equivalent of ATP, and glutamine as a nitrogen source and represents an attractive metabolic drug target. Upon the ordered binding of ATP followed by XMP to GMPS, an ester exchange reaction occurs to form the O^2-XMP-adenylate **1** (Figure 1) and inorganic pyrophosphate (*11*, *12*). Ammonia derived from GMPS-catalyzed hydrolysis of glutamine displaces AMP to provide the product, GMP. Inhibitors that modulate the ATP and glutamine binding sites in GMPS are known but, surprisingly, there is a lack of effective inhibitors that target the XMP/GMP binding site. Compounds targeting the XMP site would be expected to show selectivity for GMPS, unlike the ATP or glutamine analogues.

GMPS also represents the class I subfamily of glutamine amidotransferases. Amidotransferases contribute to the regulation of ammonia metabolism by efficiently transferring the amide nitrogen of glutamine to various substrates. These proteins share homologous amide-transfer domains and are found in several diverse metabolic pathways (*13*). The X-ray crystal structure of GMPS from *Escherichia coli* has been determined and reveals a conserved Cys-His-Glu triad in the

† This project was supported by a grant from the Purdue Cancer Center to V.J.D. (IN-17-31).

* Corresponding author: Phone (765) 494-5238; Fax (765) 494-1414. E-mail vjd@pharmacy.purdue.edu.

‡ M.L.D. and S.V.C. contributed equally to this work.

§ Present address: Department of Chemistry and Biochemistry, University of Maryland, College Park, MD 20742-2021.

[1] Abbreviations: GMPS, guanosine monophosphate synthetase; XMP, xanthosine 5′-monophosphate; CTP, cytidine 5′-triphosphate; PRPP, phosphoribosyl pyrophosphate; N^2-OH-GMP, N^2-hydroxyguanosine 5′-monophosphate; F-IMP, 2-fluoroinosine 5′-monophosphate; F-AMP, 2-fluoroadenosine 5′-monophosphate; TEP, triethyl phosphate; AMPDA, adenylic acid deaminase; HPLC, high-performance liquid chromatography; DIPEAA, diisopropylethylammonium acetate; NMR, nuclear magnetic resonance; HR FAB-MS, high-resolution fast atom bombardment mass spectroscopy; DTT, dithiothreitol; EDTA, ethylenediaminetetraacetic acid; NADH, nicotinamide adenine dinucleotide, reduced; EPPS, *N*-(2-hydroxyethyl)piperazine-*N*′-3-propanesulfonic acid; APAD, 3-acetylpyridine adenine dinucleotide.

10.1021/bi981980r CCC: $18.00
Published on Web 12/10/1998

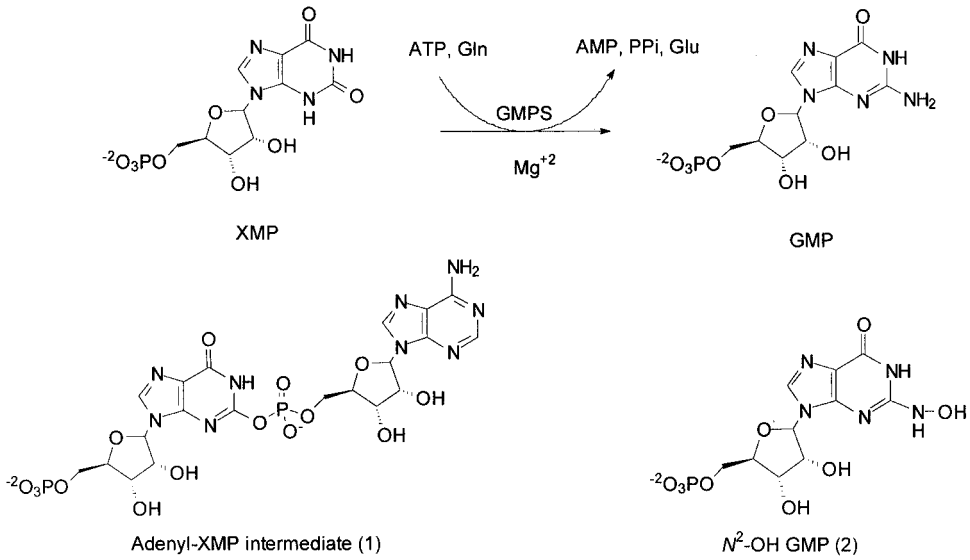

FIGURE 1: Reaction catalyzed by guanosine monophosphate synthetase. XMP, xanthosine 5′-monophosphate; ATP, adenosine 5′-triphosphate; GMP, guanosine 5′-monophosphate; Gln, L-glutamine; Glu, L-glutamate; AMP, adenosine 5′-monophosphate; PP_i, inorganic pyrophosphate; N^2-OH-GMP, N^2-hydroxyguanosine 5′-monophosphate.

glutamine catalytic site (*14*). The binding sites for ATP and glutamine have been identified; however, the structure lacks density for a strand of 22 contiguous amino acids near the AMP binding site that has been proposed to constitute the XMP binding loop. A striking feature of the current structural data is the spatial relationship between the nucleotide and glutamine active sites. The nucleotide binding and glutamine hydrolysis subdomains are separated by solvent-accessible space, implicating a substantial global conformational change for efficient ammonia transfer.

Most amidotransferases will use ammonium salts as an alternative to glutamine in vitro, albeit with reduced efficiency (*13*). Hydroxylamine is also an alternate substrate for several other glutamine amidotransferases such as asparagine synthetase, CTP synthetase, carbamoyl phosphate synthetase, and PRPP amidotransferase (*15*−*18*). However, an early investigation of GMPS substrate specificity suggested that the enzyme was inhibited by a nucleotide intermediate possibly derived from attack of hydroxylamine on the O^2-XMP-adenylate intermediate **1** (*19*, *20*). Trace amounts of a nucleotide intermediate were isolated and shown to inhibit a fresh enzyme sample, but a structural characterization was not pursued. A likely outcome of hydroxylamine attack would be N^2-hydroxyguanosine 5′-monophosphate (N^2-OH-GMP, **2**) (Figure 1). The synthesis of the nucleoside, N^2-hydroxyguanosine has been reported, but the report did not address the inhibitory activity with GMPS (*21*). Our continuing structural and mechanistic studies of GMPS have prompted the synthesis of small molecular weight probes and a resolution to the mechanism of hydroxylamine-induced inhibition.

EXPERIMENTAL PROCEDURES

Chemical reagents were purchased from standard commercial sources, including Aldrich, Fluka, and Sigma. Deionized water was distilled directly into glass before use. Triethyl phosphate (TEP, Aldrich) was purified by vacuum distillation from BaO (78 °C, 4 mmHg) and sealed in a vial under argon for storage. Reactions that were sensitive to atmospheric moisture were run under positive pressures of argon or nitrogen in flame-dried glassware with Teflon-coated stir bars. Materials were dried from H_2O by lyophilization, and temperature-sensitive materials were typically stored in a desiccator over drying agents or in sealed vials at −20 °C. Thin-layer chromatography on cellulose plates (Whatman) were developed with standard solvent systems as indicated. Visualization of the developed plates was performed by both UV absorbance at 245 nm and sulfosalicylic acid dip and ferric chloride spray followed by heating. Reverse-phase HPLC conditions were developed on a Beckman system equipped with a 128 detector, using Hamilton PRP-1 columns (4.1 × 250 mm). Mobile phases were filtered and degassed through a 0.45 μm Nylon (Alltech) filter. All the nucleotides prepared in this study were purified under ion-pairing conditions with 25 mM diisopropylethylammonium acetate, pH 7.0 (DIPEAA), and 1−2% acetonitrile as the eluent on PRP-1 (21.5 × 250 mm). Fast atom bombardment mass spectral data were obtained with the specified ionization polarity on a Kratos MS 50. NMR spectra were acquired with a Brüker ARX 300 spectrometer. Chemical shifts for ^1H and ^{13}C are listed relative to external (trimethylsilyl)propanesulfonic acid solutions in D_2O. Fluorine chemical shifts are reported relative to external trifluoroacetic acid in D_2O, while phosphorus chemical shifts are reported relative to external solutions of 85% H_3PO_4 in D_2O. XMP obtained from commercial sources was found to contain xanthosine as an impurity that contributed to a lag phase in the direct assay. Hence XMP used in the kinetic studies was purified on PRP-1 columns with 0.1% TFA in water as the mobile phase. Adenosine deaminase, lactate dehydrogenase, and glutamate dehydrogenase were purchased from Boehringer Mannheim, while pyruvate kinase and myokinase were obtained from Sigma.

Nucleotide Synthesis

*2-Fluoroinosine 5′-Monophosphate (F-IMP, **5**).* In a 15 mL screw-cap polyethylene vial, 126 mg of F-AMP (0.363 mmol) was dissolved with 6 mL of 10 mM citrate buffer (pH 6.5) at ambient temperature. To the vial were added 12

100 μL portions of 25.5 units mL^{-1} 5′-adenylic acid deaminase over 12 days at 30 °C. The reaction was monitored by reverse-phase HPLC at a flow rate of 1 mL min^{-1}, with 25 mM DIPEAA/2% CH_3CN as the eluent. The contents of the vial were lyophilized to a clear colorless oil. This oil was divided into three portions and triturated two times with 5 mL of diethyl ether before being dissolved in 3 mL of mobile phase. The mixture was separated by preparative reverse-phase HPLC on PRP-1 with a flow rate of 9.5 mL min^{-1} and the entire sample was processed in three separate injections. The product containing fractions were identified by UV scan from 200 to 300 nm, pooled, and dried by lyophilization. To remove the residual DIPEAA, the solid was redissolved in 5 mL of water and dried by lyophilization, and this process was repeated to provide 93.6 mg (84% based on recovered starting material) of a white solid: R_f 0.21 (cellulose, 3:3:3 acetonitrile/2-propanol/250 mM NH_4OH). ^{1}H NMR (300 MHz, D_2O) δ 8.29 (s, 1 H, H at C8), 5.92 (d, J = 6.11 Hz, 1 H, H at C1′) 4.90 (t, J = 5.66 Hz, 1 H, H at C2′), 4.44 (dd, J = 3.37 and 5.16 Hz, 1 H, H at C3′), 4.29 (dd, J = 3.48 and 6.02 Hz, 1 H, H at C4′), and 3.94 (ψt, J = 4.32 Hz, 2 H, H at C5′). ^{13}C NMR (75 MHz, D_2O) δ 170.98 (d, J_{C-F} = 17.9 Hz, C6), 162.52 (d, J_{C-F} = 212.8 Hz, C2), 153.13 (d, J_{C-F} = 20.6 Hz, C4), 140.6 (s, C8), 123.82 (s, C5), 88.98 (s, C1′), 87.13 (d, J_{C-P} = 8.6 Hz, C4′), 76.66 (s, C2′), 73.19 (s, C3′), and 65.97 (s, C5′). ^{31}P NMR (121 MHz, D_2O) δ 4.45 (s). ^{19}F NMR (282 MHz, D_2O) δ −22.94 (s). UV (H_2O) 254 and 265 (sh) nm. HR FABMS (−Ve, glycerol) *m*/*e* calculated for $C_{10}H_{12}FN_4O_8P$: 365.0299; found, 365.0308 [M − 1]$^-$.

*N^2-Hydroxyguanosine 5′-Monophosphate (N^2-OH-GMP, **2**).* In a 5 mL reaction vial was dissolved 15 mg (0.041 mmol) of **5** in 900 μL of H_2O. To this solution was added 70 μL of 1.45 M hydroxylamine hydrochloride in H_2O with stirring at ambient temperature. The reaction was monitored by analytical HPLC on PRP-1 with 25 mM DIPEAA/1.0% CH_3CN at a flow rate of 1 mL min^{-1}. Once the starting F-IMP **5** was consumed, the reaction was diluted with 1 mL of H_2O and dried by lyophilization. The resultant solid was then purified by semipreparative reverse-phase HPLC on PRP-1 (7 × 250 mm) with the same mobile phase at a flow rate of 3 mL min^{-1}. The fractions containing **2** were pooled, diluted to 100 mL with chilled water, and dried by lyophilization. To remove the residual DIPEAA, the residue was dissolved in H_2O and dried by lyophilization, and the process repeated to provide 7.5 mg (48%) of a white solid that was greater than 95% pure by analysis on analytical HPLC. This reaction was reproduced at least five different times on this scale and attempts to execute the synthesis on a larger scale were not pursued. ^{1}H NMR (300 MHz, D_2O) δ 8.15 (s, 1 H, H at C8), 5.89 (d, J = 5.69 Hz, 1 H, H at C1′), 4.77 (ψt, J = 5.39 Hz, 1 H, H at C2′), 4.62 (ψt, J = 4.11 Hz, 1 H, H at C3′), 4.43 (d, J = 3.3 Hz, 1 H, H at C4′), and 4.12 (ψt, J = 4.14 Hz, 2 H, H at C5′). ^{13}C NMR (75 MHz, D_2O) δ 185.4 (s,C6), 164.7 (s, C2), 155.3 (s, C4), 141.1 (s, C8), 122.1 (s, C5), 90.4 (s,C1′), 88.4 (d, J_{C-P} = 8.7 Hz, C4′), 77.9 (s, C2′), 74.6 (s, C3′), and 67.4 (d, J_{C-P} = 5.2 Hz, C5′). ^{31}P NMR (121 MHz, D_2O) δ 4.04 (s). UV (H_2O) 256 and 270 (sh) nm. HR FABMS (−Ve, glycerol) *m*/*e* calculated for $C_{10}H_{14}N_5O_9P$, 378.0451; found, 378.0430 [M − 1]$^-$.

To confirm the bond connectivities in the purine hetereocycle, 2 mg (5 μmol) of **2** in 150 μL of H_2O was added to 70 μL of a 50% Raney Ni slurry. The reaction vial was purged with H_2(g) and maintained under a static pressure of gas (balloon) for 2−3 h at ambient temperature. Reaction progress was monitored by HPLC analysis on PRP-1 with 25 mM DIPEAA/1% CH_3CN as eluent, using 5 μL samples of the reaction mixture for injection. Confirmation of the product nucleotide as GMP was made by comparison of UV−vis spectra and HPLC retention times with authentic samples.

Biochemical Analysis

The protocol for purification of the recombinant *E. coli* GMPS has been previously described (*22*). *E. coli* GMPS stock solutions were typically 0.5 mM and required dilution to 16.7 μM in 50 mM EPPS, pH 8.5, on a weekly basis. Protein concentrations were determined by the Bradford method with commercially available reagent kits (Bio-Rad) (*23*). Nucleotide concentrations were determined by UV on the basis of the known extinction coefficients of the nucleosides N^2-hydroxyguanosine ($\epsilon_{277.5}$ = 9300) and 2-fluoroinosine (ϵ_{254} = 11 900) (*21*, *24*). These were correlated to the phosphate content as determined by the method of Lanzetta et al. (*25*). All assays were conducted on a Cary 3 UV−vis spectrophotometer equipped with a temperature controller running the Varian Windows software (version 1.0). We observed that commercial preparations of XMP contained xanthosine as a impurity, which contributed to a lag phase in our assays. Purification of XMP by reverse-phase HPLC and prewarming of the assay mixture to 40 °C in the spectrophotometer before initiation of the reactions prevented this lag phase in control reactions. Substrate saturation experiments were determined over a range of 5 μM−1 mM. Substrate inhibition by XMP (K_m 14 μM) was observed at concentrations greater than 200 μM (data not shown) and hence all assay mixtures contained XMP at maximal concentration of 200 μM. Data collections were configured to acquire not less than one point every 0.1 s. Data obtained from all these experiments were analyzed by KaleidaGraph for Windows version 3.09 (Synergy Software) that uses a Levenberg−Marquardt algorithm for general curve-fitting (*26*). Steady-state kinetics constants were estimated by the shareware program HYPER (J. S. Easterby).

Standard Direct Assay (*11*). Assay mixtures of 1 mL total volume consisted of 100 mM EPPS buffer, pH 8.5, 20 mM glutamine, 2 mM ATP, 200 μM XMP, 1 mM EDTA, 100 μM DTT, 20 mM $MgCl_2$, and varied inhibitor concentrations. The mixtures were incubated for 4 min at 40 °C in a quartz cuvette before the reaction was initiated by addition of GMPS (6 nM) in 100 mM EPPS, pH 8.5. The conversion of XMP to GMP was monitored at 290 nm on a Cary 3 spectrophotometer, with an extinction coefficient of 1500 M^{-1}cm^{-1}. To analyze steady-state inhibition constants, the substrate concentration was varied from 100 μM to 1 mM for XMP and from 200 μM to 2 mM for ATP. Alternatively, a series of assays were conducted that were initiated by addition of substrate (glutamine or ATP) after a 4 min preincubation of GMPS (6 nM) and inhibitor in the same mixture as the standard assay except for omission of one component.

Data obtained from the progress curves were fit to the integrated form of the Michaelis−Menten equation, where

v_s and v_0 represent steady-state and initial velocities, respectively, and k is the first-order rate constant for the formation of product P as a function of time t. The results were analyzed by use of the equations $k_4 = kV_s/V_0$ and $k_3/k_4 = K_i/K_i^* - 1$ according to the model depicted in Figure 5 (*27*).

$$P = v_s t + (v_0 - v_s)(1 - \exp^{-kt})/k \qquad (1)$$

Preincubation Experiments. For progress curve analysis, a series of experiments were conducted where the lifetime of the enzyme−inhibitor complex was assessed as a function of added $MgCl_2$, ATP, XMP, or a combination. GMPS (1.2 μM) and N^2-OH-GMP (**2**) (1.2 μM) in a total volume of 50 μL of 50 mM EPPS, pH 8.5, were incubated for 10 min at 40 °C in the presence or absence of 20 mM $MgCl_2$, 2 mM ATP, or 1 mM XMP. A 10 μL aliquot of these solutions was then diluted into the standard assay solution and enzyme reaction was monitored over the course of 10 min at 290 nm. The final concentration of GMPS (6 nM) in these experiments was identical to those used in the reactions initiated with enzyme.

Coupled Assay (28). Assay mixtures in 1 mL total volume consisting of 100 mM EPPS buffer, pH 8.5, 20 mM glutamine, 2 mM ATP, 200 μM XMP, 100 μM DTT, 1 mM EDTA, 20 mM $MgCl_2$, 0.16 mM NADH, 1 mM phosphoenolpyruvate, 11.4 units of myokinase, 14.2 units of pyruvate kinase, 27.5 units of lactate dehydrogenase, and varied inhibitor concentrations were incubated for 4 min at 40 °C in a quartz cuvette. The reaction was initiated by the addition of GMPS (6 nM) in 100 mM EPPS, pH 8.5. The rate of AMP formation in the GMPS reaction was monitored by observing the oxidation of NADH at 340 nm; with an extinction coefficient of 6220 $M^{-1}cm^{-1}$. A factor of 2 was considered in the calculations to account for the mole of ATP used by myokinase in the coupling reaction.

Glutaminase Assay. This assay was a modification of the method of Patel et al. (*29*). The reaction mixtures were prepared as in the direct assay with 4.2 nM GMPS. The samples were incubated at 37 °C for 10 min, followed by immersion in boiling water for 2 min. The mixture was cooled to room temperature and centrifuged at 12 000 rpm in an Eppendorf microfuge for 3 min, and 250 μL aliquots of the supernatant were used to estimate the glutamate production. The coupled reaction mixtures contained 50 mM imidazole buffer, pH 8.5, 1 mM APAD, 5 mM KCl, 1 mM EDTA, and 10 units of glutamate dehydrogenase. These mixtures were incubated after addition of the sample aliquots at 30 °C for 30 min before the absorbance was measured at 363 nm. Standard curves generated for 0−500 μM glutamate were used to calculate the amount of glutamate produced in the enzymatic reaction with the lower limit of detection at 0.1% turnover of the substrate. One unit of glutaminase produces 1 μmol of glutamate/min at 37 °C.

RESULTS

Chemistry. The title compound N^2-OH-GMP (**2**) was originally planned to be synthesized by direct hydroxylamine displacement of the fluorine in 2-F-IMP (**5**) (Scheme 1). Preparation of **5** by Yoshikawa phosphorylation of 2-fluoroinosine (**4**) was anticipated to be uneventful and the synthesis was completed from guanosine by published procedures (*24*).

Scheme 1: Synthesis of **5** and **2**

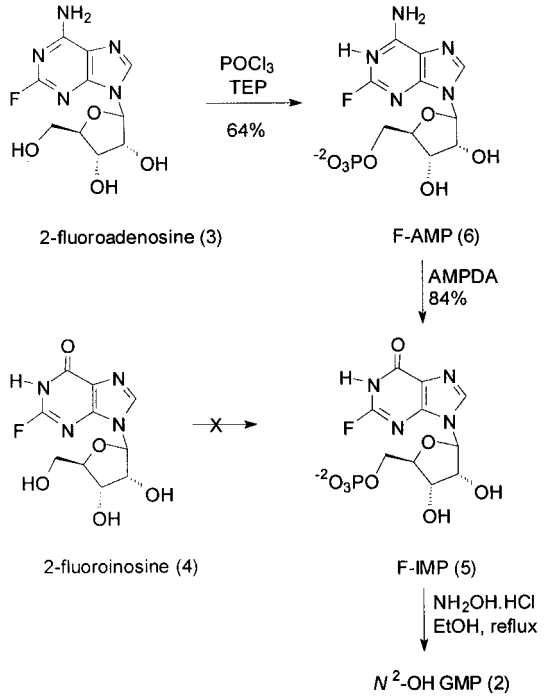

However, the phosphorylation of **4** to **5** suffered from low yields and impurities as previously noted and rendered the recovered material useless for biological evaluation (*30*, *31*).

An alternative strategy to provide **5** recruited the enzyme adenylic acid deaminase (AMPDA) to catalyze hydrolytic deamination of 2-fluoroadenosine 5′-monophosphate (F-AMP, **6**) (*32*). The commercially available enzyme cited is a partially purified preparation from *Aspergillus* that is inexpensive and convenient. F-AMP (**6**) was prepared by established procedures by phosphorylation of 2-fluoroadenosine (**3**) (*33*−*35*). Initial efforts indicated that instead of the desired product **5**, this preparation of AMPDA converted **5** to the nucleoside 2-fluoroinosine (**4**, data not shown). Control experiments with AMP confirmed that multiple activities existed in the enzyme preparation including a phosphatase (data not shown). The purified enzyme that is now commercially available has substantially reduced levels of these activities and cleanly converts **6** to **5**.

The title compound N^2-OH-GMP (**2**) was then prepared by hydroxylamine displacements of fluoride from 2-fluoroinosine 5′-monophosphate (**5**). Several related examples of displacements from 2-fluoro-6-oxopurine ribonucleosides have been reported (*36*−*39*). Initial efforts to displace fluoride with basic solutions of hydroxylamine provided equimolar amounts of the hydrolysis product, XMP, and **2**. This complication was avoided by direct use of excess hydroxylamine hydrochloride in aqueous solutions. The UV spectrum of **2** is distinctive from those of F-IMP and GMP (see Figure 2) and provides important diagnostic information about the substitution on the purine moiety. When these reactions were carefully monitored by HPLC and purified immediately, **2** was recovered as the exclusive nucleotide product. Prolonged reaction times or exposure to high pH led to some hydrolysis product XMP. The structure of **2** was confirmed by NMR and mass spectrometry and was also identified by RaneyNi reduction to guanosine 5′-monophosphate.

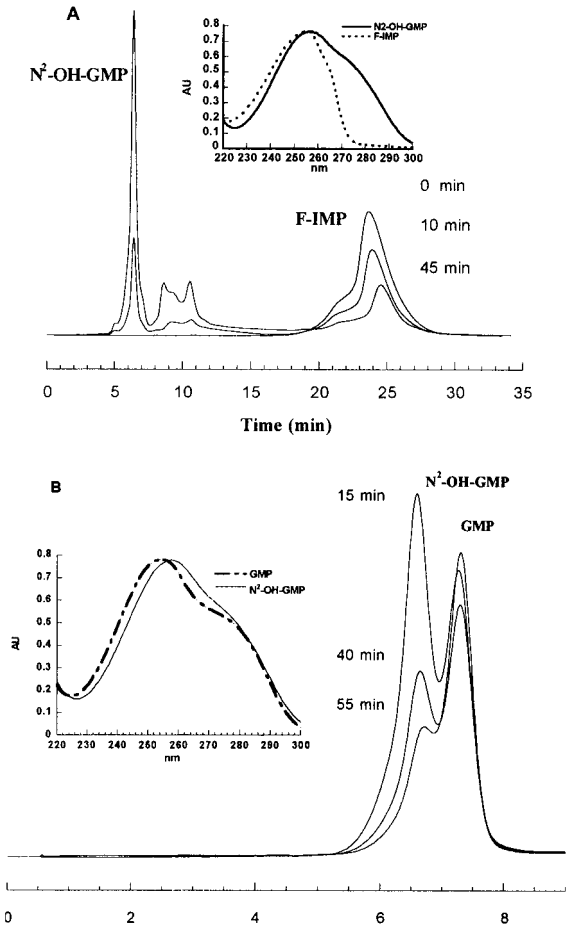

FIGURE 2: (A) Superimposed chromatograms of the conversion of **5** to **2** at 254 nm. (B) Reduction of **2** to GMP followed by HPLC and UV.

*Evaluation of **5** and **2** as Inhibitors of GMPS.*

Steady-State Analysis. Previous studies have established the intermediate adenylate **1** in the GMPS reaction and that it is not released by the enzyme during turnover (*11*, *12*). A reasonable assumption would be that GMPS must ionize the xanthosine moiety by proton removal to provide the reactive nucleophile prior to displacement of inorganic pyrophosphate from ATP by the 2-keto oxygen of XMP. Since the nucleotide **5** bears some steric and electronic similarity to this hypothetical reactive intermediate, it was tested as a steady-state inhibitor of GMPS. The C−F and C−O bond lengths and dipole moments are similar in XMP and **5**, prompting the expectation that both compounds would encounter specific binding interactions with GMPS. Inhibition studies of GMPS with **5** revealed that this compound exhibited a surprisingly low affinity for the enzyme ($IC_{50} \geq 2$ mM), while the productlike compound N^2-OH-GMP (**2**) exhibited a 10^4-fold greater affinity for GMPS ($IC_{50} = 280$ nM, data not shown). This result is in contrast to the inhibition exhibited by the product GMP ($K_i = 330$ μM) (*28*).

To establish the reaction of GMPS inhibition by **2** as a function of substrate concentrations, a glutamine initiation protocol was developed for the steady-state assays. These experiments were conducted by preincubation of GMPS with nucleotide substrates and **2** followed by reaction initiation with glutamine. Linear rates were observed over the region from 200 to 300 s and were used to estimate the steady-state velocities. The compound was found to be a reversible inhibitor with respect to XMP ($K_i = 120 \pm 20$ nM) and best fit to a competitive inhibition model. Simple variation of ATP concentrations under these conditions indicated that inhibition with respect to ATP was uncompetitive ($K_{ii} = 515 \pm 45$ nM), a result that was consistent with the ordered binding mechanism in which the inhibitor binds like the substrate XMP only after ATP.

Time Dependence and Reversibility of N^2-OH-GMP Inhibition. The primary kinetic data for N^2-OH-GMP- (**2**-) dependent inhibition of GMPS displayed significant changes in rate over the first 2−3 min; followed by a linear phase (Figure 3A), and dictated the use of steady-state noninitial velocities in the inhibition analyses above. Assays that were initiated with enzyme showed rates that decreased after the first 30 s, and the time dependence of the onset for inhibition by **2** suggested a nonclassical mechanism involving a slow-binding event (*27*). To further identify the ligands involved in the slow equilibrium, preincubation experiments with GMPS and **2** in the presence or absence of substrates and metal cofactors were conducted. Formation of the GMPS−**2** complex was enhanced by the presence of ATP (Figure 3B). In the case of these preincubation assays, the time dependence of binding equilibrium was observed as a slow recovery of enzyme activity as the inhibitor was diluted with the saturating concentrations of the substrate during the course of the assay.

Further analysis of inhibition data was performed by fitting progress curves to the integrated form of the Michaelis−Menten equation (*27*) (eq 1). The results from both substrate initiation and preincubation experiments demonstrated that the inhibition was reversible, in contrast to the observation that inhibition by hydroxylamine was apparently irreversible (*20*). An estimate of the k_{off} value was obtained from XMP initiation and preincubation experiments and allowed an estimate of k_4, the rate for dissociation of the enzyme inhibitor complex. This estimate was used to evaluate the relationship between inhibitor concentration and k_{obs} values obtained from fitting progress curves in the enzyme initiation experiments. The best fit of the data was to the hyperbolic function that describes a rate expression (eq 2) for a two-step model involving initial binding followed by a slower isomerization to a higher affinity complex (Figure 5) (*27*). In combination with the supporting kinetic data, the model in Figure 5 best describes a minimal model for the binding of **2** and substrates with GMPS. Thus **2** represents a novel inhibitor that does not bind at the ATP binding loop like decoynine and psicofuranine but presumably binds at the XMP/GMP binding site (*40*). The kinetic constants that were estimated from both the steady-state and progress curve analyses are summarized in Tables 1 and 2.

$$k_{obs} = k_4 + \left[\frac{k_3[I]}{\left(1 + \frac{[S]}{K_m}\right)K_i}\right] \qquad (2)$$

Effect on ATP Hydrolysis Activity. A second enzyme system was employed to assess the inhibitory effect of **2** on GMPS-dependent ATP hydrolysis (Figure 4A). If the rate of ATP hydrolysis increased as a function of inhibitor

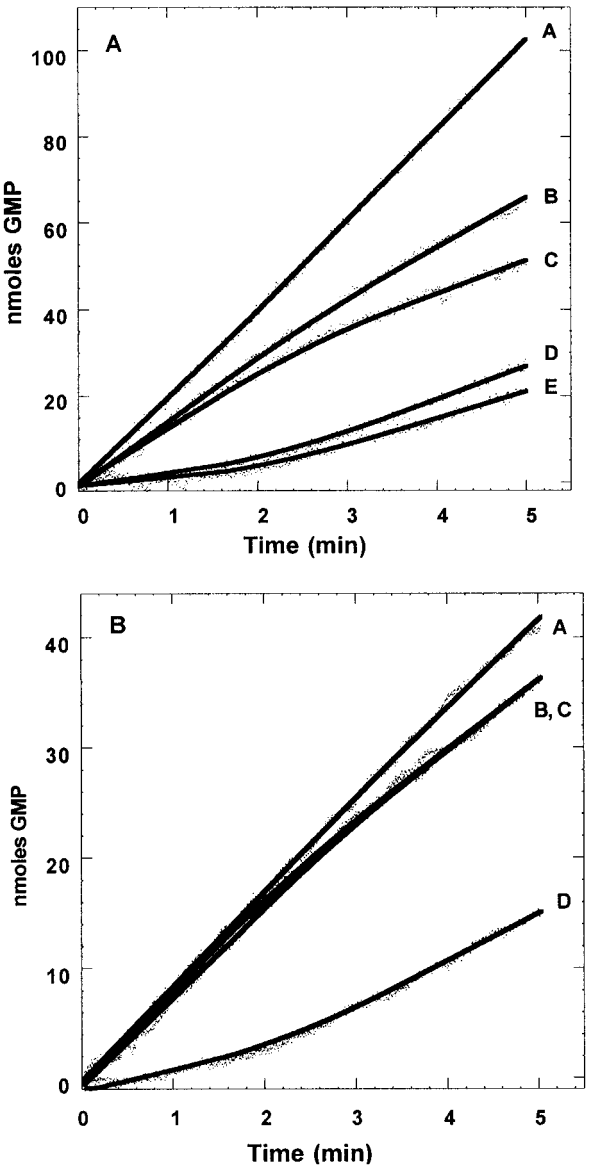

FIGURE 3: (A) Progress curves of GMPS reaction using the direct assay. Curve A represents the control reaction without inhibitor. Curves B and C represent the reaction initiated with enzyme (6 nM) at inhibitor concentrations of 500 and 750 nM, respectively. Curves D and E represent data from the reaction initiated with 200 μM XMP at inhibitor concentrations of 500 and 750 nM, respectively. (B) Preincubation of GMPS with N^2-OH-GMP and substrates. Curve A represents 10 min preincubation control of enzyme (1.2 μM) without inhibitor. Curves B and C represent preincubation of enzyme (1.2 μM) and N^2-OH-GMP (1.2 μM) in the absence and presence of 20 mM $MgCl_2$ mixture, respectively. Curve D represents preincubation of enzyme (1.2 μM) and inhibitor (1.2 μM) in the presence of 2 mM ATP and 20 mM $MgCl_2$.

concentration, it would implicate **2** as an alternate substrate for GMPS. This assay involved the myokinase-dependent recycling of AMP to ATP and detection of pyruvate reduction with NADH-dependent lactate dehydrogenase at 340 nm. Although potential kinetic limitations were perceived in the coupled systems, the assay was optimized to prevent the occurrence of any initial lag phase (*28*). No stimulation of ATPase activity was observed, indicating that the ternary complex formed, E·ATP·**2**, does not turn over. In fact, the inhibition pattern obtained from these coupled assays paralleled those obtained from the direct assays where conversion of XMP to GMP was monitored at 290 nm (Table 1).

Table 1: Steady-State Kinetic Data

	K_m	IC_{50}
XMP	14 μM[a,b]	
ATP	1 mM[c]	
Gln	1 mM[c]	
GMP		330 μM[c]
F−IMP (**5**)		>2 mM[a]
		0.28 μM[a]
N^2−OH GMP (**2**)		0.46 μM[b]
		0.30 μM[d]

[a] Direct assay. [b] Coupled ATPase assay. [c] Spector et al.(*34*) [d] Coupled glutaminase assay.

Table 2: Results of Time-Dependent Kinetic Analysis

assay	k_3[a] (min^{-1})	k_4[a] (min^{-1})	K_i (nM)	K_i* (nM)	$t_{1/2}$ (min)
enzyme initiation	0.1174	0.0911	212	92	7.19
preincubation		0.0932			7.44
glutamine initiation			120[b]		
			515[c]		

[a] See Figure 5. [b] Varied XMP. [c] K_{ii} varied ATP.

Effect on Glutaminase Activity. Adenine nucleoside inhibitors of GMPS like decoyinine and psicofuranine are analogues of adenosine and show competitive inhibition with ATP (*41*). In the presence of XMP and inorganic pyrophosphate, these compounds mimic the quaternary complex E·AMP·XMP·PP_i and stimulate glutamine hydrolysis. Our data from the preincubation experiments with **2** implicate the formation of a ternary E·ATP·**2** complex that was distinct from that of decoyinine and psicofuranine. Therefore, we decided to evaluate the effect of this ternary complex on glutamine hydrolysis. We hypothesized that binding of **2** and ATP at the active site in the synthetase domain would stimulate the glutaminase domain to hydrolyze glutamine.

The amount of glutamate produced in the enzymatic assay was monitored by a coupled end-point assay involving the reduction of 3-acetylpyridine adenine dinucleotide (APAD) in the presence of excess glutamate dehydrogenase at 363 nm (*29*). Results from these studies indicated that **2** inhibited glutamine hydrolysis with an IC_{50} = 297 nM (Figure 4B). Decoyinine, a known inhibitor of GMPS that stimulates glutaminase activity, was included as a positive control. Our results imply that the mechanism of inhibition by **2** is different from that of known nucleoside inhibitors of GMPS. These data also support the hypothesis that the ternary complex formed by **2** with GMPS and ATP is structurally different from those formed by psicofuranine and decoyinine.

DISCUSSION

While the full mechanistic details of hydroxylamine-induced inhibition of GMPS may be complex, high-affinity binding of N^2-OH-GMP (**2**) is consistent with the original hypothesis and accounts for a major portion of the effects on GMPS. On a structural basis, **2** appears as a simple analogue of the product GMP, although the details of the interaction with GMPS reveal a more complex relationship. Our study of the GMPS inhibition by **2** has established this compound as the first high-affinity inhibitor competitive with the binding of XMP. Only the product GMP and its analogues 8-aza-GMP, 6-thio-GMP, and the nucleoside antibiotic oxanosine have been previously shown to have

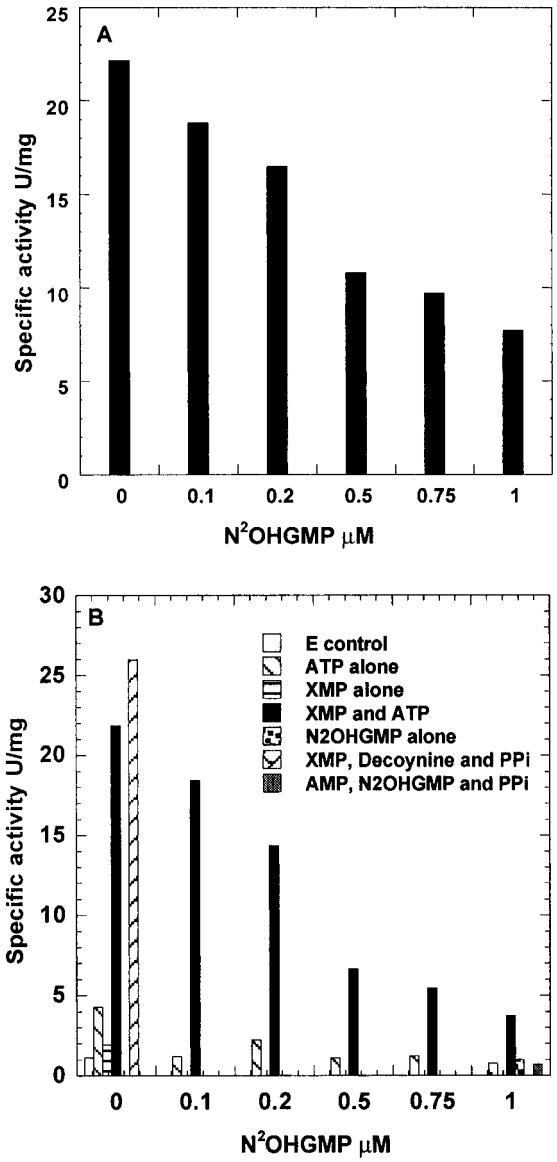

FIGURE 4: (A) Effect of N^2-OH-GMP (**2**) on ATP hydrolysis activity of GMPS. (B) Effect of N^2-OH GMP (**2**) on glutaminase activity of GMPS.

detectable inhibitory activities (K_i = 330 μM, 400 μM, 3 mM, and 740 μM, respectively) (*28*, *42*). Surprisingly, F-IMP (**5**) showed nominal inhibitory activity with GMPS. These data suggest that the functional environment on the enzyme is not arranged to recognize hydrogen-bond acceptors attached at the C2 of the 6-oxopurine nucleotide binding site. Instead, the enzyme probably promotes the development of negative charge on the oxygen that acts as a nucleophile toward the α phosphorus of ATP by shifting the equilibrium from the lactam to lactim form via tautomerization of N^3. There are additional mechanisms for interaction of **2** with GMPS that deserve consideration. For example, **2** may inhibit GMPS by specific metal ion chelation (Mg^{2+}) within the nucleotide binding site. Regardless, amine substitutions at C2 of the 2-oxopurine ribonucleotides, like GMP and the title compound **2**, are recognized by GMPS and highlights avenues for future inhibitor design.

The activity of the adenyl nucleosides, psicofuranine and decoyinine, offers an important distinction to the proposed model for GMPS inhibition by **2**. These materials bind GMPS in the presence of XMP, are competitive with ATP, and their inhibition is potentiated 30-fold by inorganic pyrophosphate (*41*). Glutaminase activity in the absence of ATP is nominal, but the psicofuranine−inorganic pyrophosphate combination stimulates glutamine turnover 1.8-fold over the GMP synthetase. Thus, XMP, inorganic pyrophosphate, and psicofuranine form a complex with GMPS that closely mimics the adenylate intermediate **1**. The high-affinity GMPS·ATP·**2** complex also occupies the nucleotide binding sites without inducing the hydrolysis of ATP or glutamine. The binding site for **2** on GMPS is, therefore, distinct from the psicofuranine site. A reasonable hypothesis does emerge from these two extreme cases that hydrolysis of ATP in normal turnover (or alternatively the mimicry of the adenyl intermediate) provides the signal to the glutamine site that initiates the glutaminase activity (*43*). The minimal kinetic model in Figure 5 is also consistent with the original observation that the inhibitory compound presumed to be **2** was equally effective on GMPS from both wild type and psicofuranine-resistant mutants (*20*).

The X-ray crystal structure of GMPS has revealed an arrangement of domains within the global structure of the enzyme (*14*). In this 2.2 Å resolution model, the amidotransferase domain is separated from the nucleotide binding domain by 30 Å of solvent-accessible volume, but GMPS is shown to efficiently transfer ammonia without detectable loss to bulk solvent (*44*, *45*). Recently, X-ray crystal structures of two amidotransferases, namely, carbamoyl phosphate synthetase and glutamine phosphoribosylpyrophosphate amidotransferase, have been solved (*46*, *47*). These structures indicate the existence of an interdomain ammonia channel that is solvent inaccessible and permits efficient transfer of the NH_3 intermediate between the two active sites. The conflicting facts have lead to the hypothesis that, in GMPS, XMP binding at a disordered loop promotes a hinge motion for closing the protein to create the channel between active sites. This hypothesis is also consistent with the ordered

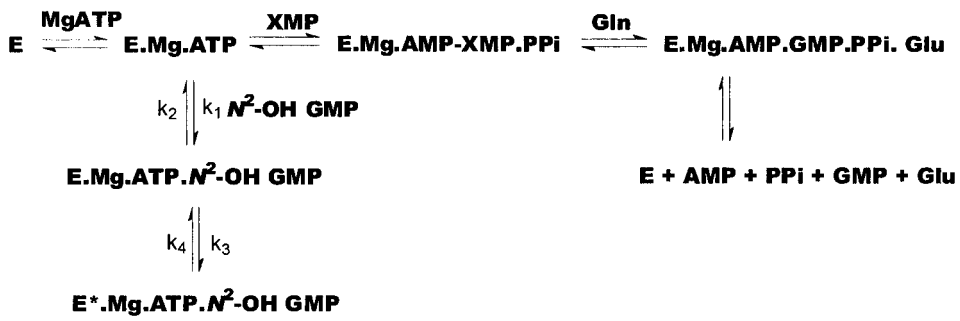

FIGURE 5: Minimal kinetic model for the inhibition of GMPS by N^2-OH-GMP (**2**).

binding of substrates and the observation that high ammonium salt concentrations are required in the absence of glutamine.

In GMPS, the structural and mechanistic features that enable the domains to relate nucleotide substrate binding to the hydrolysis of glutamine remains unclear. The time-dependent inhibitor N^2-OH-GMP (**2**) may provide some insight into the details of this challenging experimental system. The inhibition data presented here support an ordered binding of **2**, like the substrate XMP, followed by a slow isomerization to the high-affinity GMPS·ATP·**2** dead-end complex. The molecular events that promote the rearrangement to the more tightly associated species could be relevant to the conformation that lead to the O^2-XMP-adenylate intermediate **1**. Compound **2** may prove particularly useful as a conformational probe of GMPS, and an X-ray crystal structure of this enzyme−inhibitor complex could provide an important contribution in our efforts to identify a closed form of the enzyme.

ACKNOWLEDGMENT

We thank Dr. John Burgner for helpful discussions and suggestions.

REFERENCES

1. Estupinan, B., and Schramm, V. L. (1994) *J. Biol. Chem. 269*, 23068−23073.
2. Parkin, D. W. (1996) *J. Biol. Chem. 271*, 21713−21719.
3. Weber, G. (1983) *Cancer Res. 43*, 3466−3492.
4. Ohsugi, Y., Suzuki, S., and Takagaki, Y. (1976) *Cancer Res. 36*, 2923−2927.
5. Mitchell, B. S., Dayton, J. S., Turka, L. A., and Thompson, C. B. (1993) *Ann. N.Y. Acad. Sci. 685*, 217−225.
6. Fairbanks, L. D., Bofill, M., Ruckerman, K., and Simmonds, H. A. (1995) *J. Biol. Chem. 270*, 29682−29689.
7. Balzarini, J., Karlsson, A., Wang, L., Bohman, C., Horska, K., Votruba, I., Fridland, A., Aerschot, A. V., Herdewijn, P., and De Clercq, E. (1993) *J. Biol. Chem. 268*, 24591−24598.
8. Kumar, Y., Green, R., Wise, D. S., Wotring, L. L., and Townsend, L. B. (1993) *J. Med. Chem. 36*, 3849−3852.
9. Christopherson, R. I., and Lyons, S. D. (1990) *Med. Res. Rev. 10*, 505−548.
10. Sant, M. E., Lyons, S. D., Kemp, A. J., McClure, L. K., Szabados, E., and Christopherson, R. I. (1989) *Cancer Res. 49*, 2645−2650.
11. Von der Saal, W., Crysler, C. S., and Villafranca, J. J. (1985) *Biochemistry 24*, 5343−5350.
12. Fukuyama, T. T. (1966) *J. Biol. Chem. 241*, 4745−4749.
13. Zalkin, H., and Smith, J. (1998.) *Adv. Enzymol. Relat. Areas Mol. Biol. 72*, 87−144.
14. Tesmer, J. J. G., Klem, T. J., Deras, M. L., Davisson, V. J., and Smith, J. L. (1996) *Nat. Struct. Biol. 3*, 74−86.
15. Boehlein, S. K., Schuster, S. M., and Richards, N. G. (1996) *Biochemistry 35*, 3031−3037.
16. Lieberman, I. (1956) *J. Biol. Chem. 222*, 765−775.
17. McKinley, S., Anderson, C. D., and Jones, M. E. (1967) *J. Biol. Chem. 242*, 3381−3390.
18. Hartman, S. C. (1963) *J. Biol. Chem. 238*, 3024−3035.
19. Moyed, H. S., and Magasanik, B. (1957) *J. Biol. Chem. 226*, 351−363.
20. Fukuyama, T. T., and Donovan, K. L. (1968) *J. Biol. Chem. 243*, 5798−5801.
21. Long, R. A., Robins, R. K., and Townsend, L. B. (1969) *Biochim. Biophys. Acta 195*, 584−586.
22. Tesmer, J. G., Stemmler, T. L., Penner-Hahn, J. E., Davisson, V. J., and Smith, J. L. (1994) *Proteins: Struct., Funct., Genet. 18*, 395−403.
23. Bradford, M. M. (1976) *Anal. Biochem. 72*, 248−254.
24. Krolikiewicz, K., and Vorbruggen, H. (1994) *Nucleosides and Nucleotides 13*, 673−678.
25. Lanzetta, P. A., Alvarez, L. J., Remack, P. S., and Candia, O. A. (1979) *Anal. Biochem. 100*, 95−97.
26. Press, W. H., Flannery, B. P., Teukolsky, S. A., and Vetterling, W. T. (1993) *Numerical Recipes in C: The Art of Scientific Computing*, 2nd ed., Cambridge University Press, Cambridge, England.
27. Morrison, J. F., and Walsh, C. T. (1988) *Adv. Enzymol. Relat. Areas Mol. Biol. 61*, 201−301.
28. Spector, T., Miller, R. L., Fyfe, J. A., and Ketnitsky, T. A. (1974) *Biochim. Biophys. Acta 370*, 585−591.
29. Patel, N., Moyed, H. S., and Kane, J. F. (1977) *Arch. Biochem. Biophys. 178*, 652−661.
30. Antonino, L. C., and Wu, J. C. (1994) *Biochemistry 33*, 1753−1759.
31. Amarnath, V., and Broom, A. D. (1982) *Nucleosides Nucleotides 1*, 163−171.
32. Margolin, A. L., Borcherding, D. R., Wolf-Kugel, D., and Margolin, N. (1994) *J. Org. Chem. 59*, 7214−7218.
33. Yoshikawa, M., Kato, T., and Takenishi, T. (1967) *Tetrahedron Lett. 50*, 5065−5068.
34. Robins, M. J., and Uznanski, B. (1981) *Can. J. Chem. 59*, 2601−2607.
35. Robins, M. J., and Uznanski, B. (1981) *Can. J. Chem. 59*, 2608−2611.
36. Harris, C. M., Zhou, L., Stand, E. A., and Harris, T. M. (1991) *J. Am. Chem. Soc. 113*, 4328−4329.
37. Woo, J., Sigurdsson, S. T., and Hopkins, P. B. (1993) *J. Am. Chem. Soc. 115*, 3407−3415.
38. Freese, S., Hoheisel, J., Lehrach, H., and Wright, G. (1991) *Nucleosides Nucleotides 10*, 1507−1524.
39. Wang, G., and Bergstrom, D. E. (1993) *Tetrahedron Lett. 34*, 6725−6728.
40. Tesmer, J. J. G. (1995) Ph.D. Thesis, p 268, Purdue University, West Lafayette, IN.
41. Spector, T., Jones, T. E., Krenitsky, T. A., and Harvey, R. J. (1976) *Biochim. Biophys. Acta 452*, 597−607.
42. Yagisawa, N., Shimada, N., Takita, T., Ishizuka, M., Takeuchi, T., and Umezawa, H. (1982) *J. Antibiot. 35*, 755−759.
43. Nakamura, J., Straub, K., Wu, J., and Lou, L. (1995) *J. Biol. Chem. 270*, 23450−23455.
44. Truitt, C. D., Hermodson, M. A., and Zalkin, H. (1978) *J. Biol. Chem. 253*, 8470−8473.
45. Zalkin, H., and Truitt, C. (1977) *J. Biol. Chem. 252*, 5431−5436.
46. Thoden, J. B., Holden, H. M., Wesenberg, G., Raushel, F. M., and Rayment, I. (1997) *Biochemistry 36*, 6305−6316.
47. Krahn, J. M., Kim, J. H., Burns, M. R., Parry, R. J., Zalkin, H., and Smith, J. L. (1997) *Biochemistry 36*, 11061−11068.

BI981980R